

Article

The Influence of a Blade-Guiding Fin on the Pneumatic Performance of an Axial-Flow Cooling Fan

Hengtao Shu ^{1,*} and Haizhou Chen ²

¹ School of Mechanical and Automotive Engineering, South China University of Technology, Guangzhou 510641, China

² College of Electromechanical Engineering, Tsingtao University of Science & Technology, Qingdao 266042, China

* Correspondence: hengtaoshu@163.com; Tel.: +86-139-6985-2580

Abstract: An axial-flow cooling fan was taken as the research object in this paper, and a certain number of simulation models with different blade-guiding fin shapes were established. The methods of computational fluid dynamics (CFD), circumferential vorticity (CV) analysis and the response surface method (RSM) based on the design of experiments (DOE) method were all employed. The main external flow characteristics of the cooling fan, the blade surface pressure distribution, the static pressure efficiency and the fan power were obtained and compared. The relationships between the pneumatic performance and the fin shape parameters were subsequently investigated by the DOE method. The results obtained in this paper showed that a change in the fin height had a great influence on the pneumatic performance, while changes in its thickness had less of an influence. For the cooling fan studied in this paper, by adding reasonable structure-guiding fins onto the cooling fan blade, the static pressure efficiency was increased by a maximum of 7.6%. The research results have a good guiding significance regarding the structure design and optimization of axial cooling fans.

Keywords: axial-flow cooling fan; pneumatic performance; blade-guiding fin; simulation models; response surface method



Citation: Shu, H.; Chen, H. The Influence of a Blade-Guiding Fin on the Pneumatic Performance of an Axial-Flow Cooling Fan. *Machines* **2023**, *11*, 483. <https://doi.org/10.3390/machines11040483>

Academic Editor: Kim Tiow Ooi

Received: 27 February 2023

Revised: 13 April 2023

Accepted: 14 April 2023

Published: 18 April 2023



Copyright: © 2023 by the authors. Licensee MDPI, Basel, Switzerland. This article is an open access article distributed under the terms and conditions of the Creative Commons Attribution (CC BY) license (<https://creativecommons.org/licenses/by/4.0/>).

1. Introduction

Axial-flow cooling fans are an important part of the cooling systems of car engines. In order to meet the needs of high-performance air-cooled cooling systems, the development of cooling fans with a high pneumatic performance is very important. The modern research processes of cooling fans mainly include setting up a numerical simulation model through computational fluid dynamics (CFD) based on the experimental method, performing data post-processing obtained from the simulations and performing shape optimization.

In order to capture more details of fan flow fields, more and more scholars are paying attention to simulation technology (Ge et al. [1]; Ding et al. [2]; Foti [3]). Moreover, this technique can effectively reduce experimental costs, so it has been used to design and optimize the structure of cooling fans. The flow fields of cooling fans are composed of various vortices. These vortices have different sizes and vector directions that form and develop on fluid machine surfaces and are closely related to the efficiency of these machines.

Horia et al. [4] studied the boundary vorticity dynamics (BVD) theory in depth. Based on the BVD and circumferential vorticity (CV) theories, the CV distribution pattern will directly affect the flow capacity of a fan. The CV should be confined within the near-wall region as much as possible and should not be diffused into the main stream. If the flow capacity is improved and the blockage is reduced, the positive CV should occupy a larger radial position, while the negative CV should occupy a smaller radial position to improve the spatial moment. Peng et al. [5] studied the external flow field of an automobile cooling fan (ACF) and optimized the ACF shape. Lei et al. [6] employed the theory dynamics based on the physical–mathematical relationship between the flow field characteristic variables

to optimize a multi-stage axial-flow compressor and achieved considerable results. Liu et al. [7] employed the theory mentioned above to the axial-cooling fan redesign process and flow field analysis of axial-flow turbines and obtained the distribution of the negative CV on the blade surfaces. CV analysis can quickly locate the shape design defects of fluid machinery and improve the development efficiency of fluid machines by optimizing their structures.

Yoon et al. [8] explored the fundamental factors affecting the pneumatic performance of axial-flow fans and carried out a large number of experimental studies on the flow field on blade surfaces in early 2004. Parker et al. [9] demonstrated that both a positive and negative CV were distributed on the surface of low-flow axial-flow fan blades, which led to pressure gradients and induced tip leakage, finally reducing the mechanical performance. The results of Zhou et al. [10] also confirmed that the above phenomenon also existed in the flow field of turbine machinery. In order to eliminate or reduce these differences, it is necessary to change the vortex distribution by changing the blade surface structure.

Ge et al. [11] suggested that “Bionic Structures” could effectively improve the fluid dynamics performance for cooling fans. Hua et al. [12] added a “Fin-like” fin structure to the pressure surface of a turbine fan blade. The structure could guide the air flow to adapt to the complex flow field, change the vorticity distribution and blade surface pressure profile and improve tip leakage; thus, the static pressure efficiency could be improved effectively.

Jameson et al. [13] first proposed the concept of fluid mechanical structure parameterization and the optimal design of systems and successfully applied the concept in the aerospace field. However, the relationship between pneumatic performance and the design variables of the shape is manifold and complex. For example, hydrostatic efficiency is positively related to hydrostatic pressure and negatively related to the fan power. Based on this point, the design principles of cooling fans should focus on the following: decreasing the fan power and improving the static pressure lift capacity to overcome the engine cabin impedance. Therefore, it is necessary to find a kind of balanced design and an effective shape optimization method to optimize the design of fans.

Xiao et al. [14] applied the multi-objective optimization method to the optimization of the design of a squirrel cage fan and achieved positive results. In addition, Safikhani et al. [15], Abolfazl et al. [16] and Meng et al. [17] successfully applied a genetic algorithm, a neural network algorithm and RSM, respectively, to different kinds of optimization designs of fluid mechanical structures.

Among all the optimization methods mentioned above, the DOE-based RSM has the advantage of a high computational efficiency, and it can effectively avoid local optimization. In addition, the relationship between the response surface and the design variables can be applied to the optimization process of the latter. Based on the method mentioned above, Liu et al. [18] studied the relationship between the design variables and the pneumatic performances of a centrifugal fan, where the total-pressure efficiency of the fan was increased by about 5.0% after the optimization; the results were positive and effective. Therefore, the fluid mechanical structure optimization method based on DOE is feasible.

The purpose of this paper was to explore and provide a more efficient structure optimization design of an axial-flow cooling fan. During the exploration, the simulation calculation method, CV analysis method and RSM based on the DOE method were all employed. However, this method has not been widely used in the design of axial-flow cooling fans used in car engines, and this was attempted in this paper.

The research results showed that the integrated optimization method was effective. The optimal design method described above could effectively improve the pneumatic performance and shorten the R&D cycle of cooling fan.

2. Simulation Method

2.1. Research Model

Based on the ideas provided in Refs. [1–3], the 3D model of the cooling fan was built using the Catia software. During the modeling process, some unimportant hub structures

were simplified (Ding et al. [2]). On the basis of the above, a simulation model of the pneumatic performance of the cooling fan was established, which included five main areas such as the inlet, outlet, rotating domain and data-monitoring surface. Then, all the areas were meshed.

The duct simulation model was divided into five important parts, as shown in Figure 1. The inlet position variable was the volumetric flow of air, which was variable according to the experimental conditions. The outlet position variable was the atmospheric pressure in free space. The cooling fan was located in the rotating domain. The static pressure and power loss data of the fan were obtained by data post-processing. The air in the whole duct was assumed to be incompressible. If the flow rate difference between the inlet and outlet was less than 0.5%, the calculated results were considered as convergent.

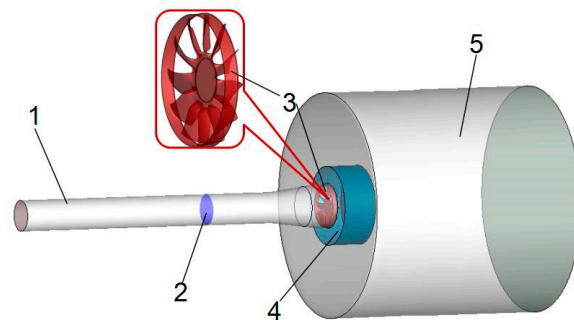


Figure 1. Simulation model of pneumatic performance of axial-flow cooling fan. 1—Inlet; 2—data monitoring surface; 3—cooling fan; 4—rotating domain; 5—outlet.

Meshing the simulation model was one of the key steps in the numerical calculation. As shown in Figure 2, hexahedral and tetrahedral meshes were chosen to reduce the computational costs. In the model, the rotating domain was meshed as a tetrahedron, and the inlet and outlet domains were meshed as hexahedrons. The $C1-\varepsilon$ and $C2-\varepsilon$ values were 1.44 and 1.92, respectively. The maximum orthogonal angle of the mesh was no greater than 75° , and the maximum extension ratio was less than 2.1, which ensured a high mesh quality. The range of the y^+ values for walls was 10.1~335.3.

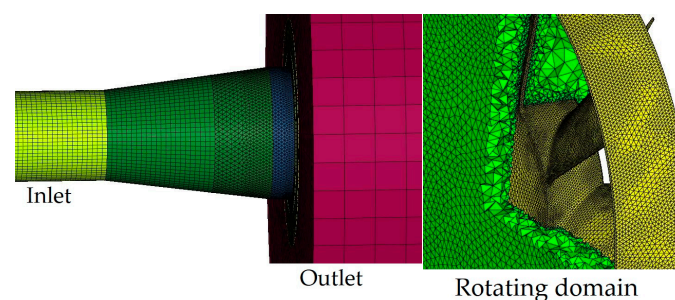


Figure 2. Mesh generation of the simulation model.

2.2. Simulation Settings

The object of this paper was a low-Mach-number axial-flow machine. In order to improve the efficiency of the calculation and the speed of the steady calculation state, in the premise of ensuring the numerical accuracy of the calculation results, the standard $k-\varepsilon$ turbulence model was applied to the simulation. The simulation process was carried out in Ansys FLUENT14.0. The setting process of the simulation process is described as follows (Ding et al. [2]):

- The fan was set in the rotating domain, and the other areas, such as inlet and outlet, were set as static.

- The default ambient temperature was 25 °C, the reference atmosphere air was steady, and its pressure was 1 atm.
- During the simulation processes, the rotation domain in which cooling fan was located was set at a 1500 r/min rotation speed. The time for one cycle was 0.04 s, the time step was set at 0.0002 s, the solution step was 1000 and 5 rounds were simulated.
- The semi-implicit method for pressure linked-equations (SIMPLE) algorithm was employed for the pressure–velocity coupling problem solution.
- The second-order upwind method was employed to discretize the continuity equation, momentum equation and dissipation rate equation.

3. Simulation Method Verification

3.1. Experimental Test Bench

In order to verify the reliability of the simulation model, it was necessary to compare and analyze the data from the tests and the numerical calculations. According to the standard of GB-T1236-2000, an appropriate type of test bench was selected and built. In this paper, a duct inlet and a free outlet of a C-type test bench was selected. The schematic is shown in Figure 3.

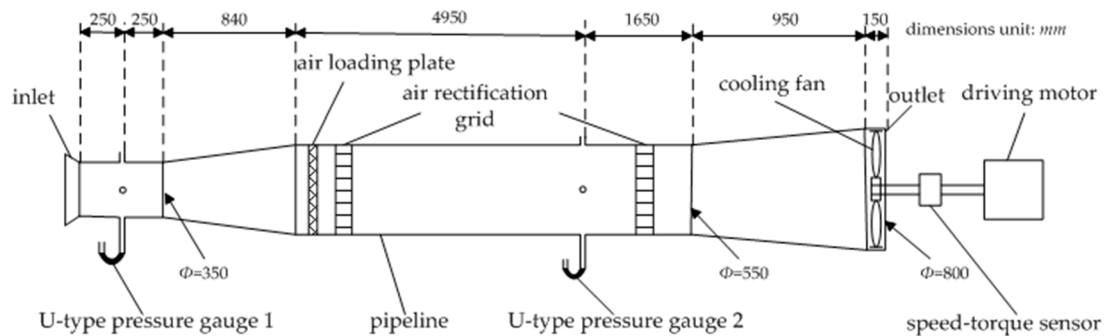


Figure 3. Schematic diagram of axial-cooling fan test bench.

The cooling fan test bench was mainly composed of an air-flow duct, a cooling fan, a driving motor and measuring instruments. Among them, the inlet duct mainly included a current collector, air-loading plates, rectification grids and U-tube liquid pressure gauges. An actual picture of the experimental device and the two tested fans (fan (a): cooling fan within guiding fins, fan (b): without fins; the other shape parameters were all the same) are shown in Figure 4, which was carried out in order to show that the pneumatic performance of the cooling fan could be effectively improved by adding guiding fins.

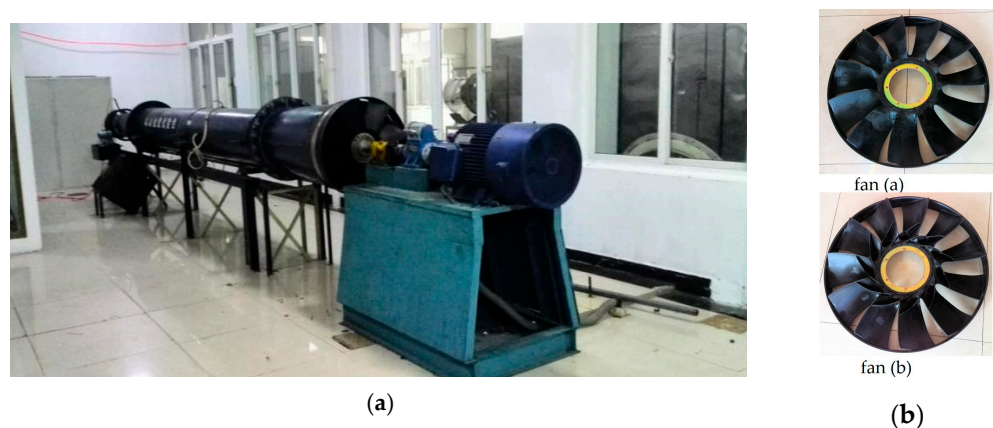


Figure 4. An actual picture of the test bench and tested fans. (a) Experimental device; (b) two different tested fans.

3.2. Experimental Results

The static pressure efficiency, η_{sp} , is an important index that is to evaluate the pneumatic performance of cooling fans. The data were calculated from the static pressure value, p_{sp} , and the input power loss value, P . The formula is expressed as:

$$\eta_{sp} = \frac{P_{st}}{P} = \frac{p_{sp}q}{P} \quad (1)$$

where P_{st} is the static pressure power (kW), which was obtained from the speed–torque sensor, P is the input power (kW), which was the total power inputted from driving motor, p_{sp} is the static pressure (Pa), which was calculated from the measured results of the U-type pressure gauge and q is the volumetric flow rate (m^3/s).

From Figure 5, it can be seen that the simulation values were close to the experimental ones. As the simulation simplified the model and neglected the power and other losses caused by the complex environment, the simulation value was higher. The maximum deviation value did not exceed 8% between the tested and calculated results. Although there were some errors, the general changing trend curves of the static pressure and efficiency were the same as each other, and the reliability of the simulation model was confirmed according to the explanation above.

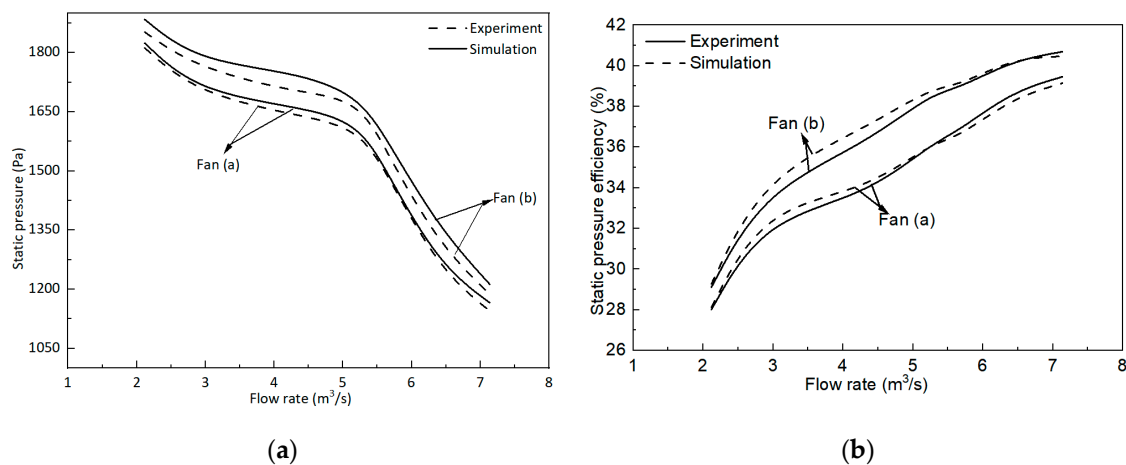


Figure 5. Calculated curves. (a) p_{sp} ; (b) η_{sp} .

4. Results and Discussion

4.1. Shape Comparison of Two Different Fans

As shown in Figure 6, the pneumatic performance of fan (b) was obviously better than that of fan (a). As shown in Figure 6a, a meridian section was selected and the velocity contour profiles near the blade surface were observed. It can be seen that the radius of the recirculation vortex was obviously reduced, and the center of the recirculation zone was further away from the blade surface. This change directly affected the vortex distribution around the fan blade. As shown in Figure 6b, both a positive and negative CV were distributed on the leaf surface. After adding the guiding fins to the blade, the area of the distribution of the negative CV was effectively reduced; thus, the average CV value was increased. For these, the air flow capacity was improved, and the pneumatic performances were both improved. The CV distribution pattern will directly affect the flow capacity of a fan. The CV should be confined within the near-wall region as much as possible and not be diffused into the main stream. If the flow capacity is improved and the blockage is reduced, the positive CV should occupy a larger radial position, while the negative CV should occupy a smaller radial position in order to improve the spatial moment.

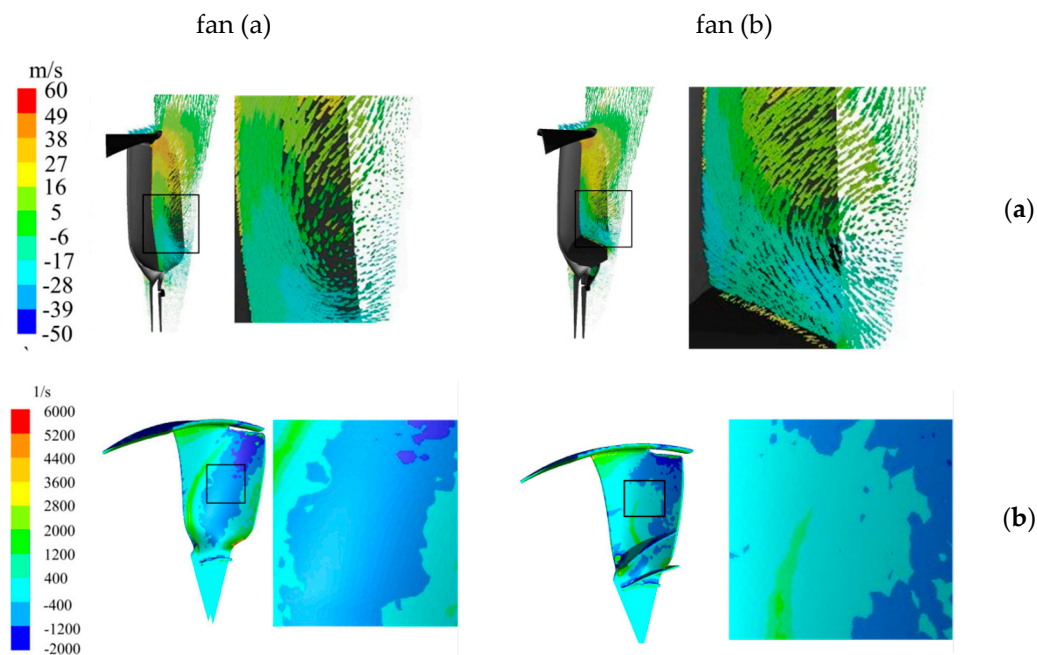


Figure 6. Flow-field characteristics of two fans. (a) Velocity contour profiles; (b) distribution of CV.

4.2. Guiding Fin Structure

As shown in Figure 7, the guiding fin was connected with two adjacent blades, and it was designed to have two distinct large areas. In addition, it comprised two shape parameters: height (H) and thickness (T). The height was defined as the distance between the upper and lower edges, as shown. The value range of the structure parameter was related to the axial projection width of the fan. The maximum value could not exceed the width value, while the minimum value was 0 mm. The guiding fin had a uniform thickness and a relatively simple definition. Its value range was related to the thickness of the blade. The specific ranges of the two shape parameters are described in the following sections.

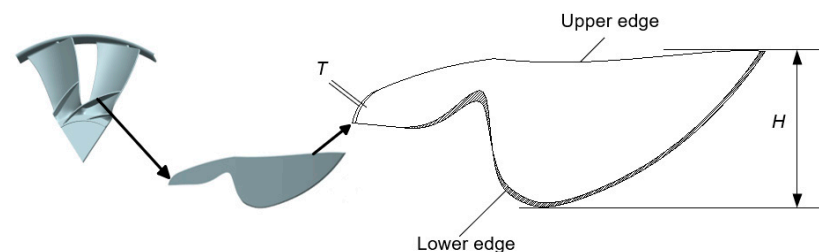


Figure 7. Geometric model of the guiding fins.

4.3. CV Distribution Affected by H

In order to observe the influence of the height of the guide fins on the pneumatic performance of the cooling fan, the CV distribution on the blade surface was obtained, as shown in Figure 8. At the same flow rate, there were different vorticity values on the blade surface, and the area of the positive CV distribution increased with the increase in the fin height. When the numerical value of the H reached a certain level, the change was no longer obvious, which was consistent with the qualitative analysis results of engineering experience.

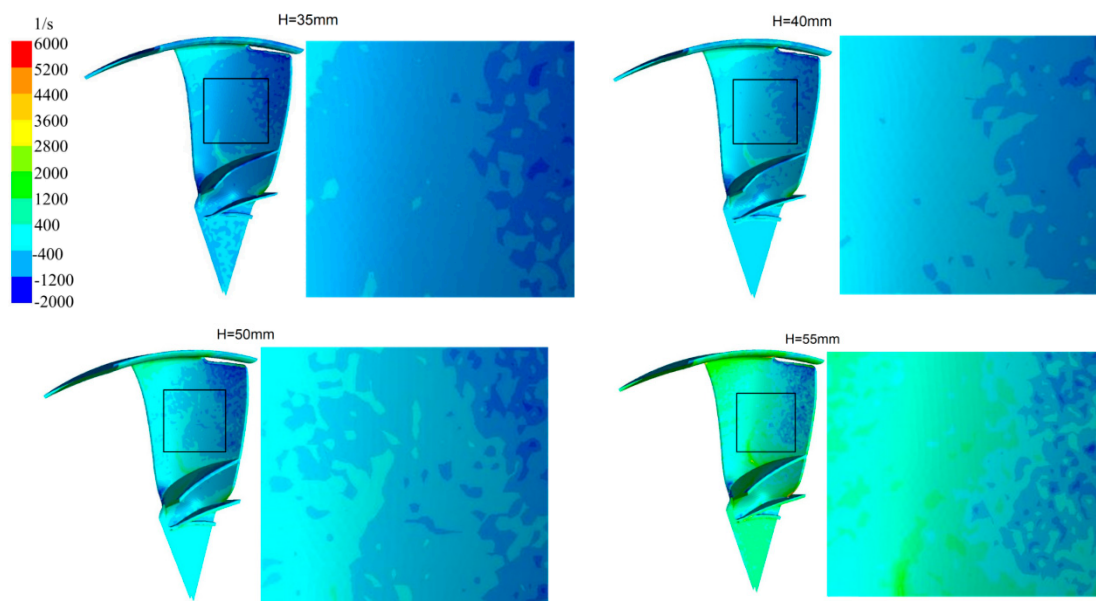


Figure 8. Distribution of CV on fan blade surface with different guiding fin heights.

4.4. CV Distribution Affected by T

The guiding fin was a kind of thin plate structure, which had a similar shape to that of a fin, and the T value was 60~90% of the thickness value of the fan blade. In this paper, it was assumed that the guiding fin had uniform thickness and no chamfering design. In order to observe the effect of the thickness of the guiding fin on the pneumatic performance of the fan, the CV distribution on the blade surface was obtained, as shown in Figure 9. At the same flow rate, the CV changed obviously only in the area near the guiding fin, but it did not change in the other areas of the blade.

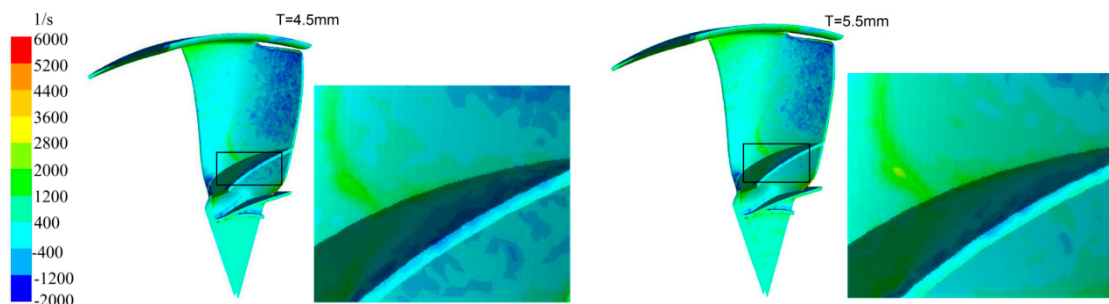


Figure 9. Distribution of CV on fan blade surface with different guiding fin thicknesses.

5. Shape Optimization

In terms of the aerodynamic performance of the cooling fan, the guiding fins could guide the air flow along the main stream, thus improving the pneumatic performance of axial-cooling fan, but the quality of the fan increased when the guiding fins were added, which meant that more driving power was required, thus increasing the power loss. Therefore, the shape parameters of the guiding fin rib cannot be designed blindly. In order to achieve the designed goal more effectively, it was necessary to introduce an efficient variable optimization design method. In this research, the RSM based on the DOE optimization method was employed to assist in the shape optimization design.

5.1. Establishing the Samples Points Space

In order to establish a more accurate proxy model, it was necessary to construct a reasonable sample points space. Considering the range of the design variables and the costs

of the calculation, an efficient sampling method based on the DOE (by the Latin hypercube method) was employed. The sample points could be distributed uniformly in the design space. The cooling fan used in this paper was mounted on an engineering vehicle with a 420 mm diameter, a 115 mm axial projection width and a 7 mm blade thickness. The height range of the guiding fin was 30~60 mm, and the thickness range was 3.0~6.0 mm. As shown in Table 1, a sample space with a capacity of 30 was created. The static pressure and power loss of all the fans were calculated by simulation, as shown in Table 2.

Table 1. Thirty sample points with different H and T values of guiding fins (mm).

No.	H	T	No.	H	T	No.	H	T
1	30.0	5.0	11	40.3	3.7	21	50.7	3.1
2	31.0	3.9	12	41.4	4.0	22	51.7	5.8
3	32.0	4.9	13	42.4	4.3	23	52.8	5.6
4	33.1	3.6	14	43.5	4.5	24	53.8	4.8
5	34.1	5.9	15	44.5	5.3	25	54.8	6.0
6	35.2	3.4	16	45.5	4.7	26	55.9	3.3
7	36.2	3.0	17	46.6	5.2	27	56.9	4.1
8	37.2	4.8	18	47.6	5.5	28	57.9	5.7
9	38.3	3.5	19	48.6	5.4	29	59.0	3.2
10	39.3	3.8	20	49.7	4.2	30	60.0	4.6

Table 2. Simulation results of 30 fans.

No.	Simulation Results			No.	Simulation Results		
	P_{sp}/Pa	P/kW	$\eta/\%$		P_{sp}/Pa	P/kW	$\eta/\%$
1	1593.2	7.6	34.0	16	1634.9	7.7	34.7
2	1604.3	7.5	34.0	17	1634.5	7.9	34.8
3	1598.1	7.6	34.1	18	1638.3	7.9	34.8
4	1607.1	7.5	34.1	19	1641.1	7.8	34.9
5	1610.2	7.6	34.1	20	1649.6	7.8	35.0
6	1607.1	7.5	34.1	21	1639.3	7.9	34.9
7	1595.1	7.5	34.0	22	1652.3	8.0	35.1
8	1608.7	7.5	34.3	23	1650.1	8.0	35.2
9	1616.7	7.5	34.3	24	1651.3	7.9	35.3
10	1622.1	7.5	34.4	25	1660.9	8.1	35.3
11	1624.5	7.5	34.4	26	1652.2	7.8	35.3
12	1627.9	7.6	34.5	27	1658.4	7.9	35.4
13	1628.9	7.6	34.6	28	1654.5	8.0	35.5
14	1631.0	7.7	34.6	29	1650.7	7.9	35.4
15	1629.3	7.8	34.7	30	1652.8	7.9	35.6

Notes: η —static pressure efficiency; fan rotating speed—1500 rpm; air flow rate—5.7 m³/s.

5.2. Establishing the RSM Model

A polynomial RSM allows for relatively complex constrained objective optimization functions to be constructed from simpler basis functions. Therefore, the polynomial RSM was used to assist in the optimization design in this paper. The mathematical relationship between the design variable, X , and the response surface function, $y(X)$, can be expressed as:

$$y(X) = \sum_{i=1}^N a_i \varphi_i(X) \quad (2)$$

where $y(X)$ symbolizes the relationship between the pneumatic performance of the axial-flow fan and the selected design variable's vector. The coefficient value i was an undeter-

mined value (i.e., could be set as 1, 2, . . . , N), which defined the number of polynomial functions. The design variables x_1 and x_2 were denoted as H and T and were expressed as:

$$y = a_0 + a_1x_1 + a_2x_2 + a_3x_1^2 + a_4x_2^2 + a_5x_1x_2 + a_6x_1^3 + a_7x_2^3 \tag{3}$$

The response surface vector variable Y can be expressed as:

$$Y = [y(X_1), y(X_2), y(X_3), \dots, y(X_L)]^T \tag{4}$$

The coefficient vector A and the basis function matrix Φ were subsequently obtained as:

$$A = (a_1, a_2, a_3, \dots, a_N)^T \tag{5}$$

$$\Phi = \begin{bmatrix} \varphi_1(X_1) & \varphi_2(X_1) & \dots & \varphi_N(X_1) \\ \varphi_1(X_2) & \varphi_2(X_2) & \dots & \varphi_N(X_2) \\ \vdots & \vdots & \vdots & \vdots \\ \varphi_1(X_L) & \varphi_2(X_L) & \dots & \varphi_N(X_L) \end{bmatrix} \tag{6}$$

$$A = (\Phi^T \Phi)^{-1} \Phi^T Y \tag{7}$$

In addition, the value of Y described in Equation (1) can be expressed in a matrix form:

$$Y = \Phi A \tag{8}$$

The results shown in Table 2 were introduced into Equation (1) and into the cubic polynomial RSM of the static pressure. The values of the power loss and the static pressure efficiency were obtained, respectively. The coefficients for each term are given in Table 3.

Table 3. RSM function terms and the corresponding coefficient values.

Terms	P_{sp}	P	η
	Coefficient Values		
1	1156	18.25	32.51
H	-20.69	-0.5931	-0.2761
T	464.0	-1.7548	3.0438
H^2	0.5639	0.0139	0.0072
T^2	-103.7	0.3766	-0.6456
HT	-0.0212	-0.0008	1.1909
H^3	-0.0044	-0.0001	-5.000
T^3	7.5721	-0.0249	0.0449

The effectiveness of response surface model functions was evaluated using the correlation coefficient (R^2), root mean square error (S_{RMSE}) and maximum relative error (Q_{MARE}). If a response surface model function has a high prediction accuracy, the above evaluation indexes should have the following characteristics: higher R^2 value, lower S_{RMSE} and Q_{MARE} value. The calculation results of the error evaluation indicators for each model are shown in the Table 4. It can be seen that the correlation coefficient of all the models was greater than 0.9, and the root mean square and maximum relative value were close to 0, which indicated that the RSM model established in this paper had a high fitness and reliability.

Table 4. Evaluation results of the RSM model.

Response Surface Model	Validation Metric		
	R^2	S_{RMSE}	Q_{MARE}
P_{sp}	0.9909	0.0147	0.0467
P	0.9176	0.0319	0.0579
η	0.9357	0.0274	0.0368

5.3. Final Shape Optimization

Based on the above research results, the fan with guiding fins had a better air flow ability. In a certain range, with the increase in the height and thickness of the fin, the pneumatic performance of the fan was improved, but the fan power loss also increased significantly. Therefore, the aim of the optimization design of the guiding fin structure is to select a height and thickness of the fin that is reasonably within the predetermined power loss range in order to greatly improve the static lift capacity of the cooling fan. Therefore, the following optimization functions are given:

$$U(H, T) = \text{Max} [P_{sp}(H, T), \eta(H, T)] \tag{9}$$

which are subject to:

$$\begin{aligned} 0 \text{ kW} &\leq P_{\text{max}}(H, T) \leq 9.0 \text{ kW} \\ 30.0 \text{ mm} &\leq H \leq 60.0 \text{ mm} \\ 3.0 \text{ mm} &\leq T \leq 6.0 \text{ mm} \end{aligned}$$

The non-dominated sorting genetic algorithm (NSGA-II, which can improve the computational efficiency and convergence) was used to solve the optimization problem described above. The sample space size was 30 and the number of iterations was set to 20, and the optimal Pareto space was obtained, which is shown in Figure 10.

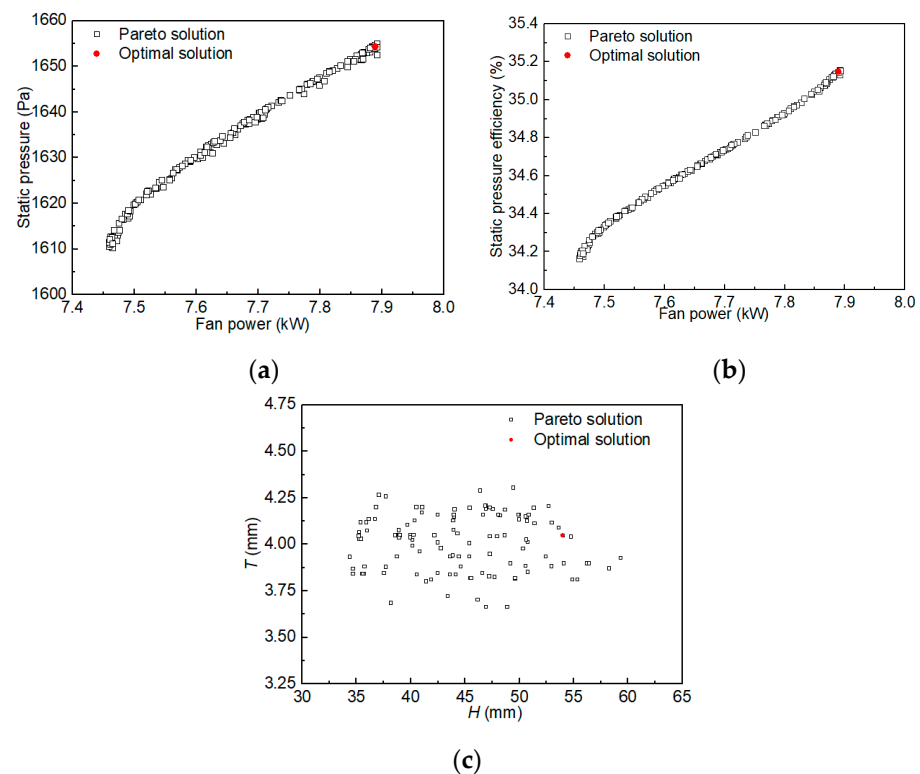


Figure 10. Pareto and optimal solutions of RSM: (a) power and static pressure; (b) power and static pressure efficiency; (c) height and thickness.

Figure 10 shows the Pareto and optimal solutions of the objective function. All the solution points did not present any functional relationship but were in the form of scattered points, which was consistent with engineering experience. After the optimization, the height and thickness values of the guiding fins were set as 51.6 mm and 4.0 mm, respectively.

5.4. Validation

In order to verify the optimization results obtained above, fans equipped with four other sets of different fin structure parameters were designed in this section for comparison. The height and thickness of the guiding fins were arbitrarily set (not belonging to any group shown in Table 1), and the shape parameter values of each are shown in Table 5. Figure 11 shows the pneumatic performance simulation results of these five fans.

Table 5. Height and thickness values of four validation guiding fins (mm).

No.	H	T
1	53.0	4.0
2	53.7	3.5
3	46.4	4.0
4	60.6	4.6

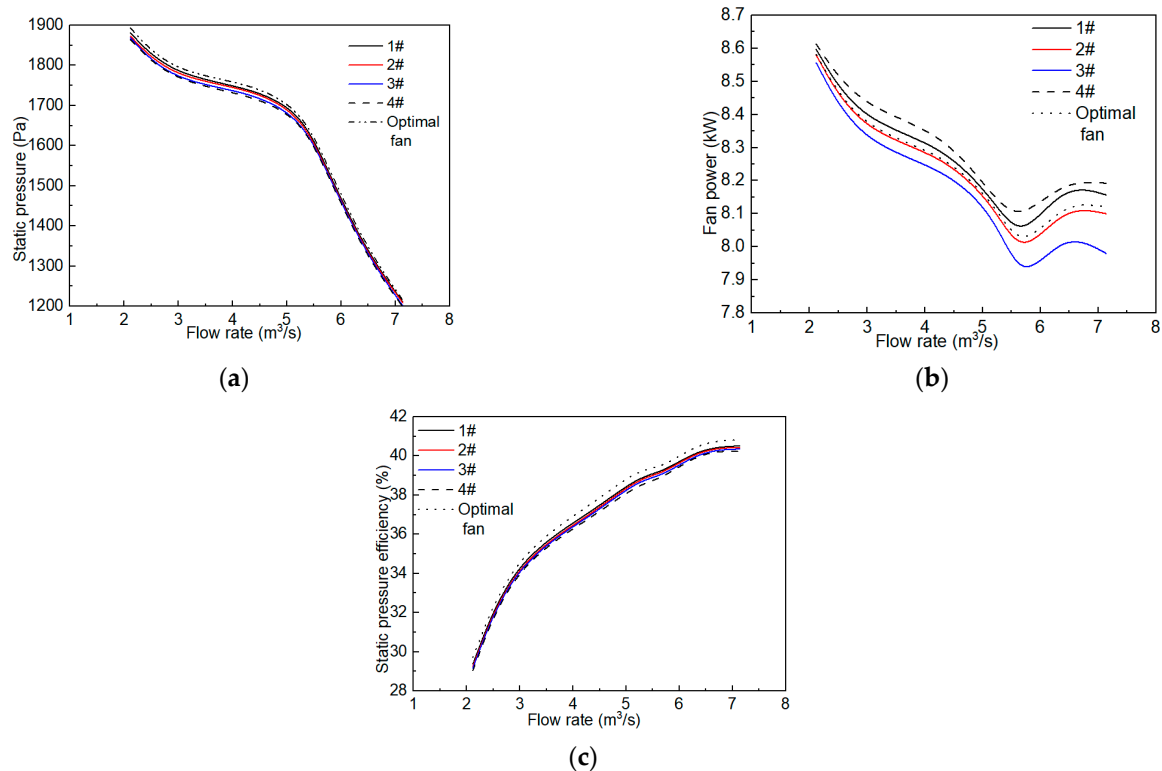


Figure 11. Simulation verification of pneumatic performances: (a) static pressure; (b) power loss; (c) static pressure efficiency.

From Figure 11, not only were the static pressure and static pressure efficiency of the fan optimized by the DOE-based RSM method both better than those of the other four fans but the power loss also did not show the worst performance. By comparing the simulation results, it was found that the fan static pressure efficiency varied from 2.1% to 3.0% when the height of the guiding fin was changed by 12.5%, and the fan static pressure efficiency varied from 2.1% to 3.0%, while the thickness of the guide fin was changed by the same value, and the static pressure efficiency varied from 0.8% to 1.9%. The results showed

that the static pressure lift capacity and the static pressure efficiency of the fan were more sensitive to variations in the height of the guiding fin.

6. Conclusions

In this paper, a simulation model of an axial-flow cooling fan with different guiding fin structures was established, and the influence of the fin height and thickness on the pneumatic performance of the fan was studied using the CFD software and the RSM method. The conclusions were as follows:

1. The pneumatic performance of the axial-flow cooling fan was related to its structure. The flow ability of the blade could be improved by adding guide fins onto the blade surface.
2. Two design variables, height and thickness, were defined in the optimization design of the guide bar structure. It was found that the pneumatic performance of the axial-flow fan was more sensitive to changes in the height of the guide fin, which provided good engineering guidance for the design of the guide fin.
3. The pneumatic performance of the fan had no direct linear relationship with the two shape variables. In order to obtain the best pneumatic performance of an axial-flow fan, the optimal range of two variables should be considered.
4. The RSM method based on DOE was creatively applied to the shape optimization design of the guide fin. Compared with the cooling fan without guiding fins, the static pressure increased by 9.5%, the power loss increased by 1.7% and the static pressure efficiency increased by 7.6% for the optimized cooling fan. The optimization results were verified to prove the feasibility of the idea.

Author Contributions: Conceptualization, methodology, software, data curation, validation and writing—original draft, H.S.; supervision and writing—review and editing, H.C. All authors have read and agreed to the published version of the manuscript.

Funding: This research was supported by Natural Science Foundation Project of Shandong province, grant number ZR2020ME124.

Institutional Review Board Statement: Not applicable.

Informed Consent Statement: Not applicable.

Data Availability Statement: Data is contained within the article.

Conflicts of Interest: The authors declare no conflict of interest.

References

1. Ge, H.W.; Norconk, M.; Lee, S.Y.; Naber, J.; Wooldrige, S.; Yi, J. PIV Measurement and Numerical Simulation of Fan-drive Flow in a Constant Volume Combustion Vessel. *Appl. Therm. Eng.* **2014**, *64*, 19–31. [[CrossRef](#)]
2. Ding, H.C.; Chang, T.; Lin, F.Y. The Influence of the Blade Outlet Angle on the Flow Field and Pressure Pulsation in a Centrifugal Fan. *Processes* **2020**, *8*, 1422. [[CrossRef](#)]
3. Foti, D. Coherent vorticity dynamics and dissipation in a utility-scale wind turbine wake with uniform inflow. *Theor. Appl. Mech. Lett.* **2021**, *11*, 266–272. [[CrossRef](#)]
4. Horia, D.; Vladimír, C.; Ion, M. Boundary Vorticity Dynamics at Very Large Reynolds Numbers. *Incas Bull.* **2015**, *7*, 89–100. [[CrossRef](#)]
5. Peng, Z.G.; Ouyang, H.; Wu, Y.D.; Tian, J. Diagnosis and Design Improvement of the Internal Flow Field in an Automotive Cooling Fan Based on Boundary Vorticity Dynamics, Part I: Blade Profile Scaling and Rotation. *J. Therm. Sci.* **2022**, *6*, 2411–2423. [[CrossRef](#)]
6. Lei, F.; Ju, Y.P.; Zhang, C. A Rapid and Automatic Optimal Design Method for Six-Stage Axial-Flow Industry Compressor. *J. Therm. Sci.* **2021**, *5*, 1658–1673. [[CrossRef](#)]
7. Liu, H.; Jiang, B.Y.; Wang, W.; Yang, X.P.; Wang, J. Redesign of Axial Fan Using Viscous Inverse Design Method Based on Boundary Vorticity Flux Diagnosis. *J. Turbomach.* **2021**, *5*, 31–42. [[CrossRef](#)]
8. Yoon, J.H.; Lee, S.J. Stereoscopic PIV Measurements of flow behind an Isolated Low-speed Axial-fan. *Exp. Therm. Fluid Sci.* **2004**, *8*, 791–801. [[CrossRef](#)]
9. Park, K.; Choi, H.; Choi, S.; Sa, Y. Effect of a Casing Fence on the Tip-leakage Flow of an Axial Flow Fan. *Int. J. Heat Fluid Flow* **2019**, *6*, 157–170. [[CrossRef](#)]

10. Zhou, Z.H.; Chen, S.W.; Li, W.H.; Wang, S.T.; Zhou, X. Experiment Study of pneumatic Performance for the Suction-side and Pressure-side Winglet-cavity Tips in a Turbine Blade Cascade. *Exp. Therm. Fluid Sci.* **2018**, *90*, 220–230. [[CrossRef](#)]
11. Ge, C.J.; Ren, L.Q.; Liang, P.; Zhang, C.C.; Zhang, Z.H. High-Lift Effect of Bionic Slat Based on Owl Wing. *J. Bionic Eng.* **2013**, *4*, 456–463. [[CrossRef](#)]
12. Hua, X.; Zhang, C.H.; Wei, J.D.; Hu, X.J.; Wei, H.L. Wind Turbine Bionic Blade Design and Performance Analysis. *J. Vis. Commun. Image Represent.* **2019**, *4*, 258–265. [[CrossRef](#)]
13. Jamseon, A. Aerodynamic design via control theory. *J. Sci. Comput.* **1988**, *3*, 233–260. [[CrossRef](#)]
14. Xiao, Q.H.; Wang, J.; Jiang, B.Y.; Yang, W.G.; Yang, X.P. Multi-objective optimization of squirrel cage fan for range hood based on Kriging model. *Proc. Inst. Mech. Eng. Part C J. Mech. Eng. Sci.* **2022**, *236*, 219–232. [[CrossRef](#)]
15. Safikhani, H.; Khalkhali, A.; Farajpoor, M. Pareto Based Multi-Objective Optimization of Centrifugal Pumps using CFD, Neural Networks, and Genetic Algorithms. *Eng. Appl. Comput. Fluid Mech.* **2011**, *5*, 37–48. [[CrossRef](#)]
16. Khalkhali, A.; Farajpoor, M.; Safikhani, H. Modeling and Multi-Objective Optimization of Forward-Curved Blade Centrifugal Fans Using CFD and Neural Networks. *Trans. Can. Soc. Mech. Eng.* **2011**, *35*, 63–79. [[CrossRef](#)]
17. Meng, F.; Dong, Q.; Wang, Y.; Wang, P.; Zhang, C. Numerical Optimization of Impeller for Backward-Curved Centrifugal Fan by Response Surface Methodology (RSM). *Res. J. Appl. Sci. Eng. Technol.* **2013**, *13*, 2436–2442. [[CrossRef](#)]
18. Liu, T.; Zhang, Y.K.; Li, K.H.; Wang, Y.; Li, J.Y. Pneumatic Optimization of a Centrifugal Fan Using Response Surface Methodology. *Open J. Fluid Dyn.* **2019**, *9*, 92–105. [[CrossRef](#)]

Disclaimer/Publisher’s Note: The statements, opinions and data contained in all publications are solely those of the individual author(s) and contributor(s) and not of MDPI and/or the editor(s). MDPI and/or the editor(s) disclaim responsibility for any injury to people or property resulting from any ideas, methods, instructions or products referred to in the content.